

Fullerene as electrical hinge

Neng Wan, Pascal Perriat, Li-Tao Sun, Qing-An Huang, Jun Sun et al.

Citation: *Appl. Phys. Lett.* **100**, 193111 (2012); doi: 10.1063/1.4714682

View online: <http://dx.doi.org/10.1063/1.4714682>

View Table of Contents: <http://apl.aip.org/resource/1/APPLAB/v100/i19>

Published by the [American Institute of Physics](#).

Related Articles

Phase separation of co-evaporated ZnPc:C60 blend film for highly efficient organic photovoltaics
APL: Org. Electron. Photonics **5**, 122 (2012)

Phase separation of co-evaporated ZnPc:C60 blend film for highly efficient organic photovoltaics
Appl. Phys. Lett. **100**, 233302 (2012)

Capacitive tunnels in single-walled carbon nanotube networks on flexible substrate
J. Appl. Phys. **111**, 063712 (2012)

Desorption of C60 upon thermal decomposition of cesium C58 fullerenes
J. Chem. Phys. **136**, 114708 (2012)

The effect of molecular impurities CO and CH4 on the structural characteristics of the C60 fullerene around the orientational phase transition
Low Temp. Phys. **38**, 221 (2012)

Additional information on *Appl. Phys. Lett.*

Journal Homepage: <http://apl.aip.org/>

Journal Information: http://apl.aip.org/about/about_the_journal

Top downloads: http://apl.aip.org/features/most_downloaded

Information for Authors: <http://apl.aip.org/authors>

ADVERTISEMENT

AIP Advances

Special Topic Section:
PHYSICS OF CANCER

Why cancer? Why physics? [View Articles Now](#)

Fullerene as electrical hinge

Neng Wan,^{1,2} Pascal Perriat,³ Li-Tao Sun,^{1,a)} Qing-An Huang,¹ Jun Sun,¹ and Tao Xu¹

¹SEU-FEI Nano-Pico Center, Key Laboratory of MEMS of Ministry of Education, School of Electrical Science and Engineering, Southeast University, 210096 Nanjing, China

²Laboratoire de Physico-Chimie des Matériaux Luminescents, Université Claude Bernard Lyon 1, UMR 5620 CNRS-UCBL, 69622 Villeurbanne Cedex, France

³Materials Engineering and Science, UMR 5510 CNRS, Université de Lyon, INSA-Lyon, 69621 Villeurbanne Cedex, France

(Received 22 March 2012; accepted 23 April 2012; published online 10 May 2012)

The current study demonstrates that fullerenes with sizes between 1.9 nm and 3.3 nm serve as an efficient electrical hinges for interconnecting sub-5 nm carbon nanotubes (CNTs). Three modes of such “soft connections” were validated via transmission electron microscopy employing *in-situ* nano-manipulation and electrical transportation measurement. A high stability of the electrical connectivity caused by the forces acting between the fullerene and nanotubes was detected. Current densities as high as $\sim 10^8$ A/cm², which almost reached the current carrier capability of CNTs, were observed within the nanocontact and a low contact resistivity ($\sim 10^{-8}$ $\Omega\cdot\text{cm}^2$) was observed between the fullerene and nanotubes. © 2012 American Institute of Physics.

[<http://dx.doi.org/10.1063/1.4714682>]

Electrical devices containing small-diameter nanowires have attracted considerable research interest because of their enhanced properties and potential application in the sensor, transistor, and solar cell fields.^{1,2} The design and optimization of the electrical connection between nanowires is one of the most important issues in such electrical devices.^{3,4} Several methods have been proposed to solve this problem. Hu *et al.*³ used the on-site growth method to connect carbon nanotubes (CNTs) and silicon nanowires by directly growing the nanowire on the tip of the CNT. Electrical measurements indicate that the contact has a rectifying property similar to a metal–semiconductor junction. Wang *et al.*⁵ fabricated interconnections between small-sized CNTs with good mechanical resilience through the deposition of amorphous carbon followed by electrical heating. Recently, Rodríguez-Manzo *et al.*⁶ proposed the e-beam irradiation of metal-filled CNTs to fabricate a two-junction CNT–metal–CNT connection, which possesses metallic conductivity and robust mechanical properties. Although all of the above methods lead to fixed interconnections with non-modifiable geometries, “soft connections” are required for designing flexible circuits that permit the relative rotations of nanowires without perturbing their electrical connectivity. Therefore, the current study proposes the idea of an “electrical hinge” (Figure 1). The prototype of this concept consists of a sphere-shaped fullerene connecting two CNTs. With this geometry, the two CNTs can support repeated bending and torsion by modifying their orientation (mode I) or distance (mode II) appropriately. In other situations, the fullerene can move along without displacement of the immobilized CNTs (mode III). An *in-situ* technique employing a STM-TEM (Nanofactory Instruments) setup was used to elaborate the prototype structure, validate the different modalities of the soft connection, and check the stability of the electrical connectivity during the motion of the so-realized “hinges.” It was demonstrated that

the “electrical hinges” those efficiently serve as “soft connections” exhibit a high current carrier capability and low interface contact resistance with the adjacent CNTs, thus, showing their potential use in carbon-based circuits.

For experiments, the multiwall CNTs were absorbed on the surface of a freshly cut Au wire with a diameter of 2 mm to elaborate *in situ* the aforementioned hinges. They were then fixed into the TEM-STM holder and inserted under a Tecnai G20 microscope in an electromagnetic shielded room (see supporting information for details⁴⁶). The CNTs had diameters varying from several nanometers to several tens of nanometers and lengths of several hundreds of nanometers (see supporting information for the CNT characterization⁴⁶). The CNT attached to the Au wire (first electrode) was driven until it connects with the counter electrode having a fixed Au tip (see supporting information⁴⁶). A large current pulse was subsequently applied to break the CNT, thus, forming graphene flakes and a small fullerene near the breaking point of the CNT. Both parts of the broken CNT were then brought into contact through the fullerene to establish the “soft connection” (i.e., the fullerene hinge: CNT–fullerene–CNT). Current–voltage (*I*–*V*) scans and images were acquired (typically, time for get one *I*–*V* curve needs <1 s) 30 min after the insertion of the holder, under a low e-beam density. These cautions permit the minimization of sample vibrations and irradiation damages. Moreover, liquid nitrogen cooling was used to decrease contamination.

Figure 2 (see supporting information for more figures⁴⁶) shows the selected TEM images of the fullerene-based connections corresponding to the three contact modes. In each mode, the CNT on the left side has an outer diameter of 3.3 ± 0.1 nm with a wall thickness of 1.2 ± 0.1 nm, which corresponds to a four- or five-layered multiwall CNT. The CNT on the right side has an average diameter of around 4.4 nm and is coated with tiny graphite flakes. The fullerene has an outer diameter of 2.5 ± 0.1 nm and a wall thickness of around 0.6 ± 0.1 nm. These dimensions are similar to those of a C₇₂₀, with a single- or double-layered structure.^{7,8} The

^{a)} Author to whom correspondence should be addressed. Electronic mail: slt@seu.edu.cn.

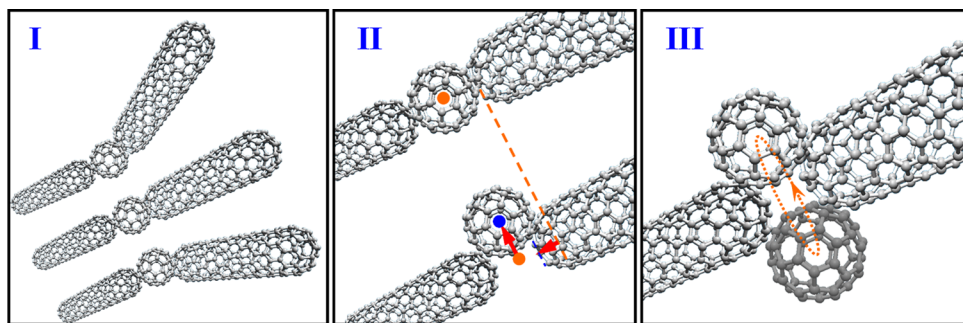


FIG. 1. Three elemental contact modes of the “electrical hinges” realized by connecting two CNTs via a fullerene. In contact mode I, the CNTs can change their relative angle by tilt and rotation. In contact mode II, the fullerene moves along the lateral direction. The orange and blue points indicate the position change of the fullerene. In contact mode III, the fullerene can rotate around the CNTs. In all modes, the connections are mechanically “soft” and the electrical connectivity is preserved. Note the CNTs and fullerene could be multilayer structures, as the situation observed in the current experiments.

contact interface between the CNT and fullerene is assumed to be circular, with an area of approximately $S = 0.8 \text{ nm}^2$ (corresponds to a contact diameter $d \sim 1.0 \text{ nm}$, estimated from direct measurement based on many TEM images. See the measurement in Fig. s4.⁴⁶). After the establishment of each connection type, an electrical solicitation was applied according to successive cycles shown in Figure 3. In mode I (“Ia” and “Ib”), the left CNT moves down the plane of the image while the fullerene position remains almost unchanged (see supporting information for the different movie illustrations⁴⁶). In mode II, the distance between the two CNTs slightly decreases from that in image “Ia” to “Ib” with the fullerene moving in the direction perpendicular to the image. In mode III (“IIIa” and “IIIb”), the fullerene moves significantly from one side of the CNTs to the other one without any CNTs motion. Interestingly, other types of motions were observed during the electrical solicitation, but all of them (more than 50 examples) can be described as a combination of these three elemental contact modes. In all cases, the physical connection was preserved during the entire electrical solicitation. This is true even if, in some experiments, the fullerene hinges underwent some carbon evaporation that led to a significant shrinkage of approximately 30% in diameter (from $2.7 \pm 0.1 \text{ nm}$ to $1.9 \pm 0.1 \text{ nm}$).

To study deeper the stability of the contact under an applied voltage, the I - V curves related to the fullerene hinges were measured using the setup detailed in the supporting information.⁴⁶ The contact stability is related to several parameters, such as the current through the contact, the temperature at the contact, and the detailed contact structure. Figure 3 shows typical I - V curves of the three elemental contact modes as shown in Figures 1 and 2. These curves are very smooth, indicating that although the connection moved in a random manner, the electrical contact between the

fullerene and CNTs was well maintained. This is certainly due to the fact that majority of the forces acting upon the connection are attractive. First is Van de Waals force (f_{vdw}),⁹⁻¹¹ which contributes attractive force and always present in nanoscale systems. The second force is related to the formation of covalent carbon bonds (CCBs) (single, double, or/and triple) between the fullerene and CNTs. This force provides additional force/energy (f_{ccb}/E_{ccb}) acting against the interface detachment. CCBs can be formed at room temperature by the migration of defects¹²⁻¹⁶ or the presence of stresses.¹⁷ During the I - V measurements, the probability of CCB formation is also highly enhanced by the temperature increase caused by the electrical heating at the vicinity of the contact.^{18,19} The third is the electrical Coulomb force (f_{ec}), which is dependent on the distance ($f_{ec} \sim d^{-2}$). When the fullerene disconnects from the CNT, opposite charges appear at the tip of the CNT and on the fullerene, immediately inducing an attracting f_{ec} (see supporting information sm5⁴⁶). Note that the charge accumulation around the electrodes was also recently observed between the electrically connected electrodes,^{20,21} suggesting that f_{ec} exists even in the case of a good physical contact between the fullerene and CNT.

In some cases, such as that of the I - V curve in Figure 3 (mode III), the electrical transportation was suddenly broken, suggesting several other possibilities that influence the stability of the fullerene hinge. The first of which could be the force caused by the random fullerene motion due to the excitation of the phonon modes by the incident electron (f_{e-h}) that has already been observed by several researchers.²²⁻²⁸ f_{e-h} occurs when a branch of the mode is excited by the injected carriers.²²⁻²⁸ This kind of force should be relatively small because of the relatively large fullerene and the small amplitude of the vibration. A more efficient effect results

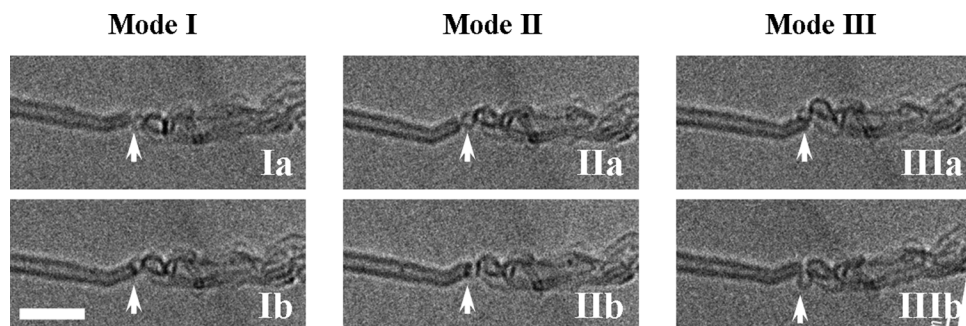


FIG. 2. TEM images of the three contact modes of the CNTs connected via a fullerene. The arrows show the different fullerene locations during electrical solicitation. In mode I (Ia and Ib), the CNT undergoes some displacement while the fullerene position remains almost unchanged. In mode II (IIa and IIb), the fullerene moves in the direction perpendicular to the image. In mode III (IIIa and IIIb), the fullerene moves from one side to the other. Bar = 10 nm.

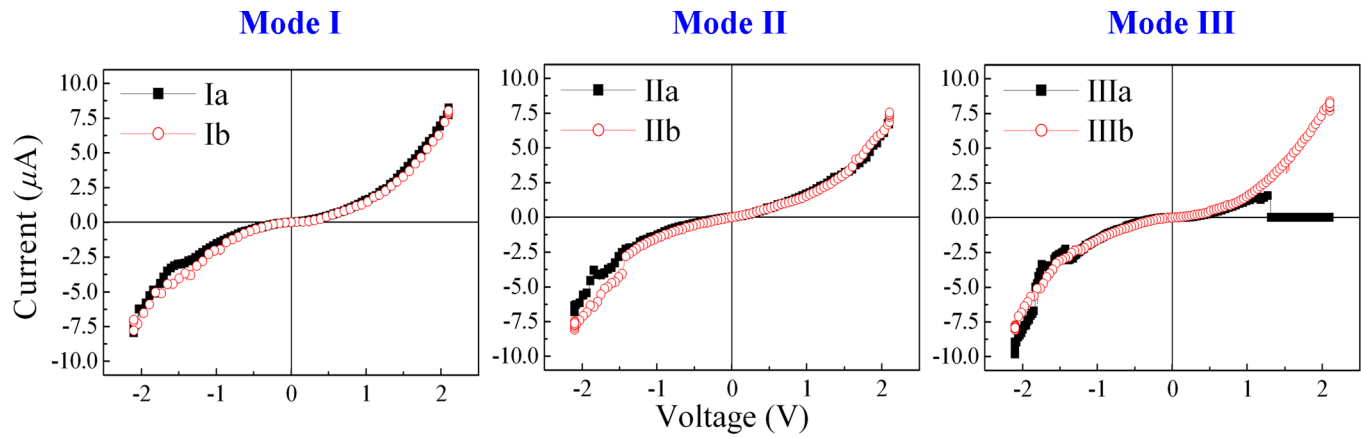


FIG. 3. The selected positively and negatively biased I - V curves of the CNT–fullerene–CNT contact. The labels correspond to the different contact geometries shown in Figure 2.

from the Lorentz force (f_{Lz}), which is created by the magnetic field of approximately 2 T that exists around the sample under the TEM microscope.²⁹ According to the geometry of the experimental setup, f_{Lz} is directly proportional to the current ($f_{Lz} \sim I$), acts perpendicularly to the CNTs,²⁹ and tends to destroy the contact. Considering that the electrical instabilities are generally observed at high currents (see Figure 3 and the movies in the supporting information⁴⁶), f_{Lz} is probably responsible for the detachment of the fullerene from the contact site. Third, the temperature increase due to the electrical heating at high currents^{30–34} can lead to the sublimation of carbon atoms^{32–34} at the vicinity of the contact site, and then cause the disconnection of the soft junction ensured by the fullerene. Although the direct relation between the interface bond broken during the I - V scan and the measured electrical instability was not established, high temperature causing CCBs loss could be an important aspect in the high temperature stability. More importantly, the large current density that flows through the small system and the deformation of the components which lead to the contact failure like in a fuse makes significance of the CCBs at the interface on the contact stability. Also, the e-beam irradiation should be considered under the current experimental set up, as the knock-off process probably causes the lost of carbon atoms at the interface and breaks the interface CCBs.^{18,19} Furthermore, It is worth to mention that the Lorentz force and the e-beam effect should be absent in ordinary applications, where the formation of CCBs between fullerene and CNTs becomes the most important aspect. As a consequence, the application of the hinge connection under a moderate current level (a contact temperature not too high) should ensure a better stability for the electrical transportation.

Under a voltage of 2 V, the current was relatively stable with a current of approximately $7 \mu\text{A}$ regardless of the connection mode of fullerene hinge. Assuming that the contact area is approximately 0.8 nm^2 , a current density of $9 \times 10^8 \text{ A/cm}^2$ passing through the fullerene could be obtained (for a current of $7 \mu\text{A}$). This density almost reaches the sustainable carrier capacity of the CNTs.³⁵ Even if the fullerene evaporates under high temperatures, the evaporation can be compensated by the formation of CCBs between the fullerene and CNTs, which insures the stable high current carrier capability.

The contact resistance between the CNT and fullerene was estimated by studying the two different configurations of a connection (Figures 4(a) and 4(b)). The geometry was verified under *in-situ* manipulation and observation in order to ensure each kind of contact and that it was not modified during the I - V curve measurements (see supporting information for methods in construction of the two kinds of contacts⁴⁶). The contact resistances between the two CNTs and between the CNT and fullerene were denoted as R_{cc} and R_{cf} respectively. Moreover, the resistance of the fullerene was assumed to be negligible. Figure 4(c) shows the equivalent

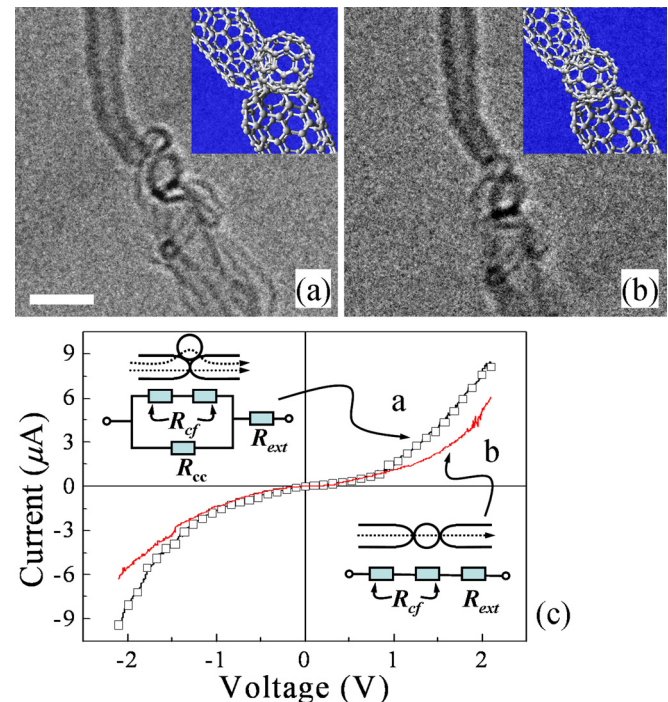


FIG. 4. Determination of the contact resistance. (a) and (b) HRTEM images of the CNT–fullerene–CNT structure under two contact configuration. The inset atom structures show the corresponding contact geometry. Bar = 5 nm. (c) Corresponding I - V curves of the CNT–fullerene–CNT structures in (a) and (b), respectively. The insets show the contact structure and equivalent electrical circuit under the two contact geometries, respectively. R_{cf} denotes the contact resistance between the fullerene and CNT, R_{cc} represents that between the two CNTs, and R_{ext} indicates the resistance relative to the rest of the circuit.

circuits of both configurations. In Figure 4(a) (the first configuration), the resistance equivalent to the soft connection can be assimilated as two serially connected R_{cf} values parallel to R_{cc} . The resistance of the whole circuit is then given as $R_{2cf//cc} = 2R_{cf}R_{cc}/(R_{cc} + 2R_{cf}) + R_{ext}$, where R_{ext} is the resistance relative to the rest of the circuit (except the connection). R_{ext} corresponds to the resistance of the CNTs themselves and the contact resistance between the CNTs and Au electrodes. In Figure 4(b) (the second configuration), the fullerene is simply serially connected to the CNTs. Thus, the resistance of the whole circuit is now given as $R_{cf/cf} = 2R_{cf} + R_{ext}$. R_{ext} is the same in both relations because all parts of the circuits (CNTs, fullerene, electrodes, and so on) are identical in both cases. Although the small gap between the two CNTs may possibly induces tunneling current, it is suggested that the tunneling current should be much smaller comparing with the contact current, thus, it is also negligible. Considering that the resistance difference between both conditions, that is $\Delta R_{cf/cf} = R_{cf/cf} - R_{2cf//cc} = 2R_{cf} [1 - R_{cc}/(R_{cc} + 2R_{cf})]$, is given by the difference in their I - V curves ($\sim 10^2$ k Ω to 10^3 k Ω under various bias voltages) and the contact resistance between the CNTs is on the order of $\sim 10^2$ k Ω to 10^3 k Ω (for reference, see also Figure s6^{46,36,37}), the contact resistance between the fullerene and CNT was also found to be on the same order, that is, $R_{cf} = \sim 10^2$ k Ω to 10^3 k Ω . As the fullerene has a contact area of approximately 0.8 nm² (smaller than its cross-sectional area of ~ 10 nm²), its contact resistivity is as low as $\sim 10^{-8}$ Ω ·cm². This value is much lower than those previously observed for CNT-metal (10^{-6} Ω ·cm²), metal-metal (10^{-5} Ω ·cm²), or CNT-semiconductor contacts (10^{-5} Ω ·cm²).³⁸⁻⁴⁰ This unexpected result was verified by more than 10 similar experiments based on the same principles.

The low contact resistance as well as the high current carrier capability between the fullerene and CNT can be attributed to two aspects. The first one is the good infiltration between the fullerene and CNTs. This infiltration, which was proven to obtain a good electrical contact between CNTs and metals such as Ti or Pd,^{39,41} is significant because the CNTs and fullerene are composed of the same carbon atoms. The second one is the formation of CCBs at the interface between the fullerene and CNTs.⁴²⁻⁴⁵ These CCBs significantly improve the contact conductance of the fullerene and CNTs, as evidenced by the unusually high densities of states near the Fermi level.⁴²⁻⁴⁵

In summary, the possibility of using fullerene as a nano-scale hinge-like connection was validated *in situ* via TEM observations using nanomanipulators and electrical transportation measurements. Fullerenes with sizes varying from 3.3 ± 0.1 nm to 1.9 ± 0.1 nm ensured a good electrical contact subjected to different connection types. These connections can be described using a combination of the three elemental contact modes. A high current density ($\sim 10^8$ A/cm²) and a low CNT-fullerene contact resistivity ($\sim 10^{-8}$ Ω ·cm²) were observed. These results indicate the promising developments of new soft electrical connections in future applications based on carbon circuits.

This work is supported by the National Basic Research Program of China (Grant Nos. 2011CB707601 and

2009CB623702), the National Natural Science Foundation of China (Grant Nos. 51071044, 60976003, and 61006011), Specialized Research Fund for the Doctoral Program of Higher Education (Grant Nos. 20100092120021 and 20100092110014) Program for New Century Excellent Talents in University (NCEF-09-0293), and Open Research Fund of State Key Laboratory of Bioelectronics. One of the author (Neng Wan) would like to give thanks to China Scholarship Council (CSC) and Fondation Franco Chinoise pour la Science et ses Applications (FFCSA) for their assistance during his staying in France.

- ¹P. G. Collins, A. Zettl, H. Bando, A. Thess, and R. E. Smalley, *Science* **278**, 100 (1997).
- ²M. P. Anantram and F. Léonard, *Rep. Prog. Phys.* **69**, 507 (2006).
- ³J. T. Hu, M. Ouyang, P. D. Yang, and C. M. Lieber, *Nature* **399**, 48 (1999).
- ⁴J. C. Charlier, X. Blasé, and S. Roche, *Rev. Mod. Phys.* **79**, 677 (2007).
- ⁵M. S. Wang, J. Y. Wang, Q. Chen, and L. M. Peng, *Adv. Funct. Mater.* **15**, 1825 (2005).
- ⁶J. A. Rodríguez-Manzo, F. Banhart, M. Terrones, H. Terrones, N. Grobert, P. M. Ajayan, B. G. Sumpter, V. Meunier, M. S. Wang, Y. Bando, and D. Golberg, *Proc. Natl. Acad. Sci. U.S.A.* **106**, 4591 (2009).
- ⁷R. R. Zope, T. Baruah, M. R. Pederson, and B. I. Dunlap, *Phys. Rev. B* **77**, 115452 (2008).
- ⁸C. Qin and L. M. Peng, *Phys. Rev. B* **65**, 155431 (2002).
- ⁹H. Ulbricht, G. Moos, and T. Herte, *Phys. Rev. Lett.* **90**, 095501 (2003).
- ¹⁰R. Tadmor, *J. Phys.: Condens. Matter* **13**, L195 (2001).
- ¹¹Y. V. Shtogun and L. M. Woods, *J. Phys. Chem. Lett.* **1**, 1356 (2010).
- ¹²S. Gorantla, S. Avdoshenko, F. Börrnert, A. Bachmatiuk, M. Dimitrakopoulou, F. Schäffler, R. Schönfelder, J. Thomas, T. Gemming, J. H. Warner, G. Cuniberti, J. Eckert, B. Büchner, and M. H. Rummeli, *Nano Res.* **3**, 92 (2010).
- ¹³M. Koshino, Y. Niimi, E. Nakamura, H. Kataura, T. Okazaki, K. Suenaga, and S. Iijima, *Nat. Chem.* **2**, 117 (2010).
- ¹⁴A. Nie, P. Wang, H. T. Wang, and S. X. Mao, *Nanotechnology* **21**, 245302 (2010).
- ¹⁵T. Z. Meng, C. Y. Wang, and S. Y. Wang, *Phys. Rev. B* **77**, 033415 (2008).
- ¹⁶C. H. Jin, K. Suenaga, and S. Iijima, *Nat. Nanotechnol.* **3**, 17 (2008).
- ¹⁷W. L. Guo, C. Z. Zhu, T. X. Yu, C. H. Woo, B. Zhang, and Y. T. Dai, *Phys. Rev. Lett.* **93**, 245502 (2004).
- ¹⁸A. V. Krasheninnikov and F. Banhart, *Nature Mater.* **6**, 723 (2007).
- ¹⁹L. Sun, F. Banhart, A. Krasheninnikov, J. A. Rodríguez-Manzo, M. Terrones, and P. M. Ajayan, *Science* **312**, 1199 (2006).
- ²⁰C. Kim and D. Jeon, *Appl. Phys. Lett.* **95**, 153302 (2009).
- ²¹L. S. C. Pingree, O. G. Reid, and D. S. Ginger, *Adv. Mater.* **21**, 19 (2009).
- ²²M. Galperin, M. A. Ratner, and A. Nitzan, *J. Phys.: Condens. Matter* **19**, 103201 (2007).
- ²³F. P. OuYang, H. Xu, and T. J. Fan, *J. Appl. Phys.* **102**, 064501 (2007).
- ²⁴S. Maier, T. L. Schmidt, and A. Komnik, *Phys. Rev. B* **83**, 085401 (2011).
- ²⁵T. Yamamoto, K. Watanabe, and S. Watanabe, *Phys. Rev. Lett.* **95**, 065501 (2005).
- ²⁶F. Haupt, T. Novotný, and W. Belzig, *Phys. Rev. Lett.* **103**, 136601 (2009).
- ²⁷A. N. Pasupathy, J. Park, C. Chang, A. V. Soldatov, S. Lebedkin, R. C. Bialczak, J. E. Grose, L. A. K. Donev, J. P. Sethna, D. C. Ralph, and P. L. McEuen, *Nano Lett.* **5**, 203 (2005).
- ²⁸J. S. Seldenthuis, H. S. J. van der Zant, M. A. Ratner, and J. M. Thijssen, *ACS Nano* **2**, 1445 (2008).
- ²⁹V. V. Volkov, D. C. Crew, Y. Zhu, and L. H. Lewis, *Rev. Sci. Instrum.* **73**, 2298 (2002).
- ³⁰G. Romano, A. Gagliardi, A. Pecchia, and A. D. Carlo, *Phys. Rev. B* **81**, 115438 (2010).
- ³¹G. Schulze, K. J. Franke, A. Gagliardi, G. Romano, C. S. Lin, A. L. Rosa, T. A. Niehaus, Th. Frauenheim, A. Di Carlo, A. Pecchia, and J. I. Pascual, *Phys. Rev. Lett.* **100**, 136801 (2008).
- ³²J. Y. Huang, F. Ding, B. I. Yakobson, P. Lu, Q. Liang, and J. Li, *Proc. Natl. Acad. Sci. U.S.A.* **106**, 10103 (2009).
- ³³J. Y. Huang, S. Chen, S. H. Jo, Z. Wang, D. X. Han, G. Chen, M. S. Dresselhaus, and Z. F. Ren, *Phys. Rev. Lett.* **94**, 236802 (2005).
- ³⁴J. Y. Huang, F. Ding, K. Jiao, and B. I. Yakobson, *Phys. Rev. Lett.* **99**, 175503 (2007).

- ³⁵Z. Yao, C. L. Kane, and C. Dekker, *Phys. Rev. Lett.* **84**, 2941 (2000).
- ³⁶A. Buldum and J. P. Lu, *Phys. Rev. B* **63**, 161403(R) (2001).
- ³⁷M. P. Garrett, I. N. Ivanov, R. A. Gerhardt, A. A. Puretzky, and D. B. Geoghegan, *Appl. Phys. Lett.* **97**, 163105 (2010).
- ³⁸T. Kawano, D. Christensen, S. P. Chen, C. Y. Cho, and L. W. Lin, *Appl. Phys. Lett.* **89**, 163510 (2006).
- ³⁹S. C. Lim, J. H. Jang, D. J. Bae, G. H. Han, S. W. Lee, I. S. Yeo, and Y. H. Lee, *Appl. Phys. Lett.* **95**, 264103 (2006).
- ⁴⁰C. Koechlin, S. Maine, R. Haidar, B. Trétout, A. Loiseau, and J. L. Pelouard, *Appl. Phys. Lett.* **96**, 103501 (2010).
- ⁴¹V. Vitale, A. Curioni, and W. Andreoni, *J. Am. Chem. Soc.* **130**, 5848 (2008).
- ⁴²C. D. Pemmaraju, I. Rungger, X. Chen, A. R. Rocha, and S. Sanvito, *Phys. Rev. B* **82**, 125426 (2010).
- ⁴³A. A. Shokri and Sh. Nikzad, *J. Appl. Phys.* **110**, 024303 (2011).
- ⁴⁴G. Y. Tu, D. P. Guo, B. R. Li, and H. L. Zhang, *Physica B* **406**, 2138 (2011).
- ⁴⁵J. Heurich, J. C. Cuevas, W. Wenzel, and G. Schön, *Phys. Rev. Lett.* **88**, 256803 (2002).
- ⁴⁶See supplementary material at <http://dx.doi.org/10.1063/1.4714682> for experimental setup, TEM images of the fullerene hinges, analysis of the I-V curves, movies, etc.